Perfect Spin Filter by Periodic Drive of a Ferromagnetic Quantum Barrier

Daniel Thuberg,[1] Enrique Muñoz,[1] Sebastian Eggert,[2,*] and Sebastián A. Reyes[1]
[1]Instituto de Física and Centro de Investigación en Nanotecnología y Materiales Avanzados, Pontificia Universidad Católica de Chile, Casilla 306, Santiago 22, Chile
[2]Physics Department and Research Center OPTIMAS, University of Kaiserslautern, D-67663 Kaiserslautern, Germany
(Received 27 July 2017; published 29 December 2017)

We consider the problem of particle tunneling through a periodically driven ferromagnetic quantum barrier connected to two leads. The barrier is modeled by an impurity site representing a ferromagnetic layer or a quantum dot in a tight-binding Hamiltonian with a local magnetic field and an ac-driven potential, which is solved using the Floquet formalism. The repulsive interactions in the quantum barrier are also taken into account. Our results show that the time-periodic potential causes sharp resonances of perfect transmission and reflection, which can be tuned by the frequency, the driving strength, and the magnetic field. We demonstrate that a device based on this configuration could act as a highly tunable spin valve for spintronic applications.

DOI: 10.1103/PhysRevLett.119.267701

Using and controlling spin degrees of freedom in electronic circuits hold much promise for future devices [1]. Such spintronic applications require spin-dependent transport and spin polarized currents, but ordinary ferromagnet-semiconductor interfaces are known to be inefficient for this purpose [2]. Spin filters have been proposed using quantum dots [3], spin orbit coupling [4], hybrid structures [5], or even DNA [6]. Lateral periodic structures can theoretically achieve 100% spin-filter efficiency based on Bragg reflection at a given energy interval [7], but they are difficult to realize and are not easily tunable. In this Letter we now show that a *time-periodic* modulation of an ordinary local gate voltage not only leads to a perfect spin-filter mechanism but also enables highly tunable and even switchable devices.

Specifically, we study the transmission of electrons through a ferromagnetic quantum barrier with an oscillating driven gate potential and connected to two leads, as illustrated in Fig. 1. We consider current excitations of opposite spin in a generic band structure modeled by a tight-binding chain with nearest neighbor hopping amplitude J. A periodically driven gate with angular frequency ω and amplitude μ is imposed upon the quantum barrier at the central site together with a local magnetic field B. The possibility of a local electron-electron interaction of strength U and a local potential energy ϵ_d on the barrier is also included. The resulting Hamiltonian reads ($\hbar = 1$)

$$H = -J\sum_{i,\sigma}(c^{\dagger}_{i,\sigma}c_{i+1,\sigma} + c^{\dagger}_{i+1,\sigma}c_{i,\sigma}) + \sum_{\sigma}[\epsilon_d - \mu\cos(\omega t) - \sigma b]c^{\dagger}_{0,\sigma}c_{0,\sigma} + Un_{0,\uparrow}n_{0,\downarrow} \quad (1)$$

in standard notation where $b = (\mu_B/2)B$. Local driving has recently become of interest in the literature [8–13]. Remarkably, single particle transmission through a periodically driven impurity without a magnetic field can give rise to sharp resonances, where the transmission vanishes completely—even for infinitesimally small driving amplitudes [12,13]. We now show that the addition of a magnetic field and the local potential energy not only make the transmission spin dependent but also cause an entirely new effect of *perfect transmission* for special parameters. The combination of such ballistic transmission and total reflection for different spin-dependent parameters therefore opens the possibility of constructing a perfect spin filter, which may be very attractive for spintronic applications.

To calculate the transmission probability for each spin channel, we will find steady-state solutions to the Schrödinger equation

$$[H(t) - i\partial_t]|\Psi(t)\rangle = 0 \quad (2)$$

using the Floquet formalism [14] for a time-periodic Hamiltonian of the form $H(t) = H_0 + 2H_1\cos(\omega t)$, as in Eq. (1). The steady-state solution is a so-called Floquet state $|\Psi(t)\rangle = e^{-i\epsilon t}|\Phi(t)\rangle$, which can be determined by the eigenvalue equation

$$[H(t) - i\partial_t]|\Phi(t)\rangle = \epsilon|\Phi(t)\rangle, \quad (3)$$

where $|\Phi(t)\rangle = |\Phi(t + 2\pi/\omega)\rangle$ is time periodic and ϵ is the quasienergy. Using the spectral decomposition

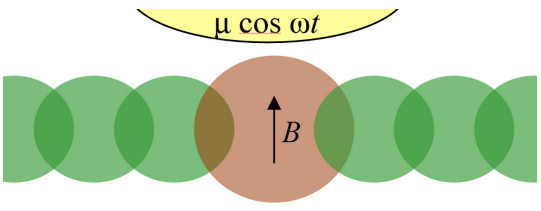

FIG. 1. Schematic setup of a ferromagnetic quantum barrier subjected to a periodic drive and connected to two leads.

$$|\Phi(t)\rangle = \sum_{n=-\infty}^{\infty} e^{-in\omega t}|\Phi_n\rangle, \tag{4}$$

the eigenvalue equation becomes

$$H_0|\Phi_n\rangle + H_1(|\Phi_{n+1}\rangle + |\Phi_{n-1}\rangle) = (\epsilon + n\omega)|\Phi_n\rangle. \tag{5}$$

The repulsive Coulomb interaction U on the barrier induces many-body correlations, which are technically difficult to deal with even in thermal equilibrium. As we show in the Supplemental Material [15], it is possible to develop a mean-field approach for Floquet systems by using a time-dependent density on the barrier $\langle n_{0,\sigma}\rangle$ such that $n_{0,\uparrow}n_{0,\downarrow} \approx \langle n_{0,\uparrow}\rangle n_{0,\downarrow} + \langle n_{0,\downarrow}\rangle n_{0,\uparrow} - \langle n_{0,\uparrow}\rangle\langle n_{0,\downarrow}\rangle$. In this way it is possible to use a general single particle state with spin σ, which is defined by the coefficients for all modes of the spectral decomposition,

$$|\Phi_n^\sigma\rangle = \sum_j \phi_{j,n}^\sigma c_{j,\sigma}^\dagger|0\rangle, \tag{6}$$

where $|0\rangle$ is the vacuum state. Inserting Eq. (6) into the eigenvalue equation (5) results in recursion relations for the amplitudes $\phi_{j,n}$. For the bulk ($j \neq 0$) we have

$$-J(\phi_{j-1,n}^\sigma + \phi_{j+1,n}^\sigma) = \bar{\epsilon}_{n,\sigma}\phi_{j,n}^\sigma, \tag{7}$$

where

$$\bar{\epsilon}_{n,\sigma} = \epsilon + U\beta_{n,\sigma} + n\omega. \tag{8}$$

Here, we have defined a mean-field parameter $\beta_{n,\sigma} = \sum_m \nu_{m,\sigma}\nu_{n-m,\bar{\sigma}}$ and $\nu_{m,\sigma} = \sum_n \phi_{0,n}^{\sigma *}\phi_{0,n+m}^\sigma$, using the notation $\bar{\sigma} = -\sigma$. In contrast to ordinary mean-field calculations, it is essential that the density on the driven quantum barrier is time dependent [15]. This has the interesting consequence that all Floquet modes become coupled at the quantum barrier for $j = 0$:

$$-J(\phi_{-1,n}^\sigma + \phi_{1,n}^\sigma) - \frac{\mu}{2}(\phi_{0,n+1}^\sigma + \phi_{0,n-1}^\sigma) + U\sum_m \nu_{m,\bar{\sigma}}\phi_{0,n-m}^\sigma = (\bar{\epsilon}_n - \epsilon_d + \sigma b)\phi_{0,n}^\sigma. \tag{9}$$

The time-periodic potential in the quantum barrier is not energy conserving and can cause scattering into other Floquet modes n. For an incoming wave with wave number k_0 for the mode $n = 0$ with quasienergy $\bar{\epsilon} = -2J\cos k_0$, the solution of Eq. (7) has the form

$$|\Phi_n^\sigma\rangle = \sum_{j<0}[\delta_{n,0}Ae^{ik_0 j}c_{j,\sigma}^\dagger + e^{-ik_n j}r_{n,\sigma}c_{j,\sigma}^\dagger]|0\rangle + \sum_{j>0} e^{ik_n j}t_{n,\sigma}c_{j,\sigma}^\dagger|0\rangle + E_{n,\sigma}c_{0,\sigma}^\dagger|0\rangle, \tag{10}$$

where the wave numbers are given by $-2J\cos k_n = \bar{\epsilon} + n\omega$. If $|\bar{\epsilon} + n\omega| < 2J$, k_n is real and the corresponding plane wave solutions are delocalized over the entire chain (unbound channels), which is always the case for the incoming wave $n = 0$. For modes with $\bar{\epsilon} + n\omega < -2J$, $k_n = i\kappa_n$ is imaginary and the solutions decay exponentially around the impurity (bound channels). For $\bar{\epsilon} + n\omega > 2J$ the solutions decay and oscillate with a complex wave number $k_n = i\kappa_n + \pi$. Using Eq. (7) it can be seen that

$$E_{n,\sigma} = t_{n,\sigma} = r_{n,\sigma} + \delta_{n,0}A, \tag{11}$$

capturing the inversion symmetry of the lattice with respect to $j = 0$. Inserting the amplitudes $\phi_{j,n}^\sigma$ that arise after Eq. (11) back into Eq. (9), we obtain a recursive relation for the coefficients $E_{n,\sigma}$:

$$E_{n+1,\sigma} + E_{n-1,\sigma} = -\frac{4iJ}{\mu}\sin k_n(E_{n,\sigma} - A\delta_{n,0}) + \frac{2}{\mu}U\gamma_n - \frac{2}{\mu}\sigma(b - \sigma\epsilon_d)E_{n,\sigma}, \tag{12}$$

which is the central equation that needs to be solved by requiring the convergence $E_{|n|\to\infty} \to 0$. Here, the influence of the interaction is captured by the term $\gamma_{n,\sigma} = \sum_m \nu_{m,\sigma}\phi_{0,n-m}^{\bar{\sigma}}$, which obviously depends on the total density of particles with opposite spin and can be iteratively determined self-consistently. In the following, we assume an unpolarized incoming current composed of equal amplitudes for opposite spin.

For the transmission coefficient, it is useful to observe that the current of the incoming wave (normalized to $|A|^2\sin k_0$) has to equal the sum of all outgoing waves,

$$\sum_n (|r_{n,\sigma}|^2 + |t_{n,\sigma}|^2)\sin(k_n) = A^2\sin(k_0). \tag{13}$$

Therefore, the total transmission can be expressed in terms of the solution for $E_{n,\sigma}$,

$$T_\sigma = \frac{1}{A^2}\sum_n T_{n,\sigma} = \frac{1}{A^2}\sum_n |E_{n,\sigma}|^2\frac{\sin(k_n)}{\sin(k_0)} = \frac{\mathrm{Re}E_{0,\sigma}}{A} = \mathrm{Re}\left[\frac{u_k}{u_k - \frac{i\mu}{2}\left(\frac{E_{1,\sigma}}{E_{0,\sigma}} + \frac{E_{-1,\sigma}}{E_{0,\sigma}}\right) - i\sigma\tilde{b}_\sigma}\right], \tag{14}$$

where we have used Eq. (12) for $n = 0$ in the last line, with $u_k = 2J\sin k_0$ as the incoming particle velocity and

$$\tilde{b}_\sigma = b - \sigma(\epsilon_d + U\gamma_{0,\sigma}/E_{0,\sigma}). \tag{15}$$

Let us first consider the effect of a magnetic field b without interactions $U = 0$ and for vanishing on-site energy $\epsilon_d = 0$, as shown in Fig. 2 as a function of the incoming energy $-2J < \epsilon < 2J$. Since the results are the same for $\epsilon \to -\epsilon$ and $\tilde{b}_\sigma \to -\tilde{b}_\sigma$, only the energy range of the upper half of the band is shown. Maybe the most striking features are the points of complete reflection $T = 0$ at certain energies ϵ. For $b = 0$ these reflection points were

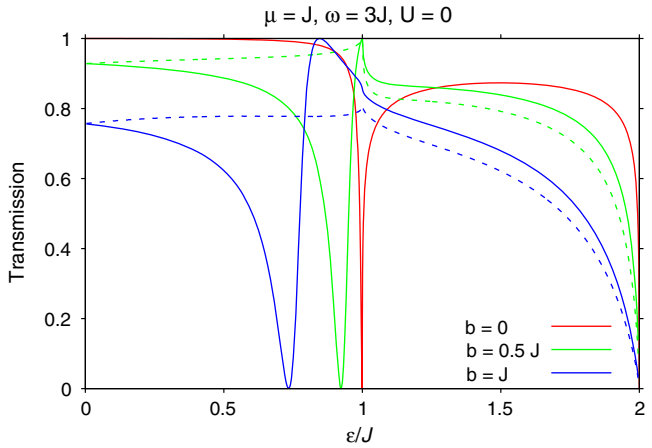

FIG. 2. Transmission (solid line, spin-up; dashed line, spin-down) for a perturbation with $\omega = 3J$, $\mu = J$ and various magnetic field strengths b as a function of ϵ. The interaction is turned off ($U = 0$) and $\epsilon_d = 0$.

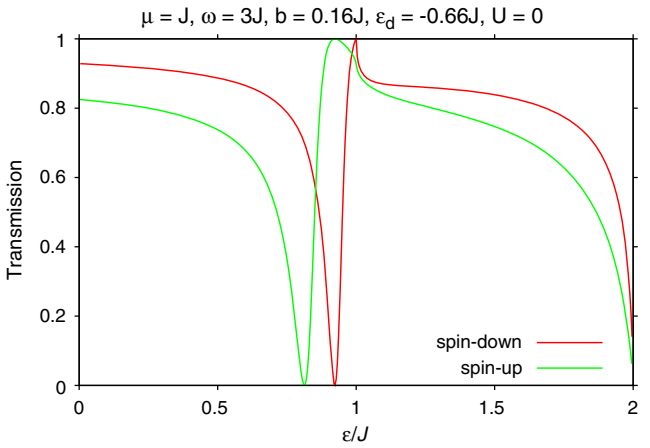

FIG. 3. Transmission behavior of both spin channels for a perturbation with $\hbar\omega = 3J$, $\mu = J$, a magnetic field strength $b = 0.16J$, and a constant potential $\epsilon_d = -0.66J$ showing the possibility for a perfect spin filter.

linked to the phenomena of Fano resonances and are known to occur even for arbitrary small driving amplitudes $\mu \to 0$ at incoming energies $\epsilon \to \omega - 2J$ [12,13]. For $\sigma b < 0$ there are no such resonances, but for $\sigma b > 0$ the points of perfect reflection now shift to lower energies and we observe a new feature of perfect transmission at nearby incoming energies, which opens the possibility of constructing a perfect spin filter, as outlined below. To estimate the locations of the zero transmission resonances, it is instructive to consider the recurrence relation in Eq. (12) for $n \neq 0$, which can be written as $E_{n+1,\sigma} + E_{n-1,\sigma} = \alpha_n E_{n,\sigma}$, where

$$\alpha_n = \frac{2}{\mu}\left[-\mathrm{sgn}(n)\sqrt{(\epsilon + n\omega)^2 - 4J^2} - \sigma\tilde{b}_\sigma\right]. \quad (16)$$

For small driving amplitudes $\mu \to 0$, the α_n values grow beyond bounds, but a resonance condition $E_{0,\sigma}/E_{-1,\sigma} \to 0$ in Eq. (14) is still possible for $\alpha_{-1} \to 0$, so that the points of zero transmission are given by

$$\epsilon \xrightarrow{\mu\to 0} \omega - \sqrt{4J^2 + \tilde{b}_\sigma^2} \quad (17)$$

for $\sigma b > 0$. As mentioned above there are corresponding resonances for $\epsilon \to -\epsilon$ and reversed spin (or field). However, if the frequency is too small or the field is too large, so that the expression in Eq. (17) becomes negative, the resonances are pushed outside the band and there will be no points of zero transmission for any energy. On the other hand, for any given incoming energy ϵ in the band, it is possible to find a sufficiently high frequency so that Eq. (17) can be fulfilled.

The points of perfect transmission $T = 1$ in Fig. 2 are also linked to the Fano resonance, which has been studied for static side coupled systems [16]. In our case the effective magnetic field $\sigma\tilde{b}_\sigma$ in Eq. (15) leads to a finite Fano asymmetry parameter and therefore a nearby point of perfect transmission. Basically, the reduced Zeeman energy enhances the local occupation at the impurity site and increases transmission through the barrier. This effect can also be achieved by a local potential energy ϵ_d as an additional tuning parameter. Specifically, it is straightforward to choose a negative value of ϵ_d and a small positive value of b, so that the effective on-site energy $\sigma\tilde{b}_\sigma$ is attractive for both spin channels but resulting in a spin-dependent shift in Eq. (17). In Fig. 3 the parameters $b = 0.16J$ and $\epsilon_d = -0.66J$ were chosen so that the transmission maximum for spin-up occurs at the same energy as the resonance of perfect reflection for spin-down. This demonstrates that it is possible to create a perfect spin filter by a combination of a static magnetic field and a local time-periodic potential.

In the high frequency regime $\omega \gg J, \tilde{b}_\sigma$, the coefficients α_n in Eq. (16) can be expanded to first order in ω^{-1}. The resulting (approximate) recurrence relation has an exact solution in terms of Bessel functions of the first kind $\mathcal{J}(x)$ [13,17]. Thus, in this regime we can obtain an analytical approximation for the transmission

$$T_\sigma \approx \frac{u_k^2}{u_k^2 + [\frac{\mu}{2}\chi(\mu/\omega) + \sigma\tilde{b}_\sigma]^2}, \quad (18)$$

where $\chi(\mu/\omega) = [\mathcal{J}_{1-\epsilon/\omega-\sigma\tilde{b}_\sigma/\omega}(\mu/\omega)]/[\mathcal{J}_{-\epsilon/\omega-\sigma\tilde{b}_\sigma/\omega}(\mu/\omega)] - [\mathcal{J}_{1+\epsilon/\omega+\sigma\tilde{b}_\sigma/\omega}(\mu/\omega)]/[\mathcal{J}_{\epsilon/\omega+\sigma\tilde{b}_\sigma/\omega}(\mu/\omega)]$. A comparison between this approximation and the exact result is shown in Fig. 4, which already coincide almost perfectly for $\omega = 10J$. Moreover, a first-order expansion of $\chi(\mu/\omega)$ in $\epsilon + \sigma\tilde{b}_\sigma$ leads to an analytic estimate for the location of the point of perfect transmission $T_\sigma = 1$ at $\mathcal{J}_0(\mu/\omega)^2 = \sigma\tilde{b}_\sigma/\epsilon + 1$. We see that tuning of the resonance locations is, therefore, equally possible by changing μ or ω.

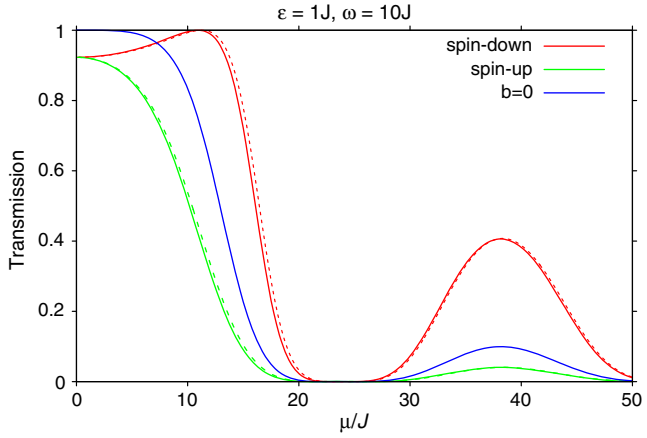

FIG. 4. Transmission of both spin channels for a perturbation with $\omega = 10J$ and a magnetic field of $b = 0.5$ as a function of μ. The interaction is turned off ($U = 0$) and $\epsilon_d = 0$. The dashed lines correspond to the approximation from Eq. (18).

Last but not least, the effect of interactions where $U \neq 0$ must be considered. As can be seen in Eq. (15), the main effect comes from the renormalization of the effective magnetic field $\tilde{b}_\sigma$ through a spin-dependent contribution to the local potential energy $\epsilon_d + U\gamma_{0,\sigma}/E_{0,\sigma}$ in the mean-field approximation. Therefore, a similar effect as seen in Fig. 3 is observed in this case, where two independent Fano resonances appear for each spin channel. The position of the resonances is approximately given by Eq. (17), with a small shift in comparison with the noninteracting case, which is self-consistently calculated within the mean-field approximation through the parameter $U\gamma_{0,\sigma}/E_{0,\sigma}$. We notice that, at high frequency ω and small amplitudes μ, the occupation of the Floquet coefficients $n \neq 0$ becomes negligible, and hence in this limit one has $U\gamma_{0,\sigma}/E_{0,\sigma} \sim U\langle n_{0,\sigma}\rangle$, such that the effective site energy is approximately $\epsilon_d + U\langle n_{0,\sigma}\rangle$, which is precisely the Hartree-Fock expression for a static impurity subject to a local interaction [18,19]. This is consistent with the interpretation following Eq. (18) that, in the very high frequency regime, the oscillations can be averaged and effectively described by *static* fields and local potentials [12,17]. In particular, using an effective field on the barrier $b_{\mathrm{eff}} = \tilde{b}_\sigma + \sigma(\mu/2)\chi(\mu/\omega)$ gives the same high frequency transmission coefficient $T = b_{\mathrm{eff}}^2/(u_k^2 + b_{\mathrm{eff}}^2)$; i.e., the local potential must simply be shifted by $(\mu/2)\chi$.

It should be pointed out that the interacting model without driving has also been of interest for studying the Kondo effect [20] using semiconductor quantum dots or single-molecule transistors [21–24]. Recently, the nonequilibrium steady-state conductance as a function of a constant bias voltage has been of considerable interest [25–33]. The oscillating potential now offers the different type of steady state discussed above. At the same time the Kondo effect comes into play if the states in the barrier are degenerate at low temperatures and finite U, which is not captured by the mean-field approach. Future research may therefore show an interesting interplay between the Kondo effect and Floquet states in this system.

The experimental implementation of such a perfect spin filter is not limited to a quasi-one-dimensional setup with the central quantum dot shown in Fig. 1 since the effect can also be derived in the same way for any system where the transport channels go through a ferromagnetic layer with a tunable time-periodic potential. A solid-state device requires relatively high frequencies on the order of the incoming energy, which is normally the Fermi energy relative to the band edge. Therefore, systems with low filling, small hopping, or large effective mass are most promising in this respect. Ferromagnetic dots on the nanoscale have been produced by laser irradiation [34] and by the proximity effect [35]. Using corresponding experimental values for the density of $n_{2\mathrm{D}} = 2 \times 10^{11}/\mathrm{cm}^2$ [34], we arrive at a Fermi energy of $\epsilon_F = \pi\hbar^2 n_{2\mathrm{D}}/m_e \sim 0.5$ meV for 2D electrons. The corresponding driving frequency of more than 100 GHz to find the resonance is certainly a challenge, but measurements [36] and tunable oscillators [37] in this range have been reported. Driving of magnetic layers with terahertz radiation has also been suggested [38] to modify systems with even larger bandwidths. In experimental systems temperatures will also play an important role since the energy spread of the incoming current will be broadened by the finite-temperature Fermi-Dirac distribution. In order for the spin filter to work, it is therefore essential that the temperature must be less than the width of the resonance, which is more than an order of magnitude smaller than the driving frequency in our simulations. Using the experimental numbers from above, we arrive at a width of about 0.05 meV or $T \lesssim 0.5$ K.

Much progress has also been made in quantum simulators using ultracold gases, where periodically driven tight-binding systems can be realized with optical lattices and cold atom systems [39]. These types of systems have provided an exciting scenario, not only as experimental simulations of solid-state models but also to test configurations with potential new features [39–47].

In conclusion, we have analyzed the effect of a local time-periodic potential on the transport through a ferromagnetic quantum barrier including local potentials, fields, and interactions. In contrast to static gating and filtering mechanisms, the periodic drive allows points of perfect transmission and complete reflection, which is useful for the generation of tunable spin currents. To achieve complete reflection for spin-down and perfect transmission for spin-up as shown in Fig. 3, two parameters must be tuned, such as the local static potential and the driving frequency.

D. T. acknowledges financial support from CONICYT Grant No. 63140250, E. M. acknowledges financial support from Fondecyt (Chile) Grant No. 1141146. S. E.

acknowledges support from the Deutsche Forschungsgemeinschaft (DFG) via the collaborative research centers SFB/TR173 and SFB/TR185.

*Corresponding author.
eggert@physik.uni-kl.de

[1] For a review, see I. Žutić, J. Fabian, and S. Das Sarma, Spintronics: Fundamentals and applications, Rev. Mod. Phys. **76**, 323 (2004).
[2] G. Schmidt, D. Ferrand, L. W. Molenkamp, A. T. Filip, and B. J. van Wees, Fundamental obstacle for electrical spin injection from a ferromagnetic metal into a diffusive semiconductor, Phys. Rev. B **62**, R4790(R) (2000).
[3] P. Recher, E. V. Sukhorukov, and D. Loss, Quantum Dot as Spin Filter and Spin Memory, Phys. Rev. Lett. **85**, 1962 (2000).
[4] T. Koga, J. Nitta, H. Takayanagi, and S. Datta, Spin-Filter Device Based on the Rashba Effect Using a Nonmagnetic Resonant Tunneling Diode, Phys. Rev. Lett. **88**, 126601 (2002).
[5] P. LeClair, J. K. Ha, H. J. M. Swagten, J. T. Kohlhepp, C. H. van de Vin, and W. J. M. de Jonge, Large magnetoresistance using hybrid spin filter devices, Appl. Phys. Lett. **80**, 625 (2002).
[6] B. Göhler, V. Hamelbeck, T. Z. Markus, M. Kettner, G. F. Hanne, Z. Vager, R. Naaman, and H. Zacharias, Spin selectivity in electron transmission through self-assembled monolayers of double-stranded DNA, Science **331**, 894 (2011).
[7] J. Zhou, Q. W. Shi, and M. W. Wu, Spin-dependent transport in lateral periodic magnetic modulations: Scheme for spin filters, Appl. Phys. Lett. **84**, 365 (2004).
[8] W. Berdanier, M. Kolodrubetz, R. Vasseur, and J. E. Moore, Floquet Dynamics of Boundary-Driven Systems at Criticality, Phys. Rev. Lett. **118**, 260602 (2017).
[9] A. Agarwala and D. Sen, Effects of interactions on periodically driven dynamically localized systems, Phys. Rev. B **95**, 014305 (2017); Effects of local periodic driving on transport and generation of bound states, Phys. Rev. B **96**, 104309 (2017).
[10] M. Moskalets and M. Büttiker, Floquet scattering theory of quantum pumps, Phys. Rev. B **66**, 205320 (2002).
[11] A. K. Eissing, V. Meden, and D. M. Kennes, Renormalization in Periodically Driven Quantum Dots, Phys. Rev. Lett. **116**, 026801 (2016); Functional renormalization group in Floquet space, Phys. Rev. B **94**, 245116 (2016).
[12] S. Reyes, D. Thuberg, D. Perez, C. Dauer, and S. Eggert, Transport through an AC driven impurity: Fano interference and bound states in the continuum, New J. Phys. **19**, 043029 (2017).
[13] D. Thuberg, S. A. Reyes, and S. Eggert, Quantum resonance catastrophe for conductance through a periodically driven barrier, Phys. Rev. B **93**, 180301 (2016).
[14] M. Griffoni and P. Hänggi, Driven quantum tunneling, Phys. Rep. **304**, 229 (1998).
[15] See Supplemental Material at http://link.aps.org/supplemental/10.1103/PhysRevLett.119.267701 for a derivation of the mean-field ansatz for Floquet systems.
[16] A. E. Miroshnichenko and Y. S. Kivshar, Engineering Fano resonances in discrete arrays, Phys. Rev. E **72**, 056611 (2005).
[17] G. Della Valle, M. Ornigotti, E. Cianci, V. Foglietti, P. Laporta, and S. Longhi, Visualization of Coherent Destruction of Tunneling in an Optical Double Well System, Phys. Rev. Lett. **98**, 263601 (2007).
[18] A. C. Hewson, Renormalized Perturbation Expansions and Fermi Liquid Theory, Phys. Rev. Lett. **70**, 4007 (1993).
[19] A. C. Hewson, *The Kondo Problem to Heavy Fermions* (Cambridge University Press, Cambridge, England, 1993).
[20] J. Kondo, Resistance minimum in dilute magnetic alloys, Prog. Theor. Phys. **32**, 37 (1964).
[21] D. Goldhaber-Gordon, J. Göres, M. A. Kastner, H. Shtrikman, D. Mahalu, and U. Meirav, From the Kondo Regime to the Mixed-Valence Regime in a Single-Electron Transistor, Phys. Rev. Lett. **81**, 5225 (1998); D. Goldhaber-Gordon, H. Shtrikman, D. Mahalu, D. Abusch-Magder, U. Meirav, and M. A. Kastner, Kondo effect in a single-electron transistor, Nature (London) **391**, 156 (1998).
[22] G. D. Scott, Z. K. Keane, J. W. Ciszek, J. M. Tour, and D. Natelson, Universal scaling of nonequilibrium transport in the Kondo regime of single molecule devices, Phys. Rev. B **79**, 165413 (2009).
[23] G. D. Scott, D. Natelson, S. Kirchner, and E. Muñoz, Transport characterization of Kondo-correlated single-molecule devices, Phys. Rev. B **87**, 241104(R) (2013).
[24] M. L. Perrin, E. Burzurí, and H. S. van der Zant, Single-molecule transistors, Chem. Soc. Rev. **44**, 902 (2015).
[25] Z. Iftikhar, S. Jezouin, A. Anthore, U. Gennser, F. Parmentier, A. Cavanna, and F. Pierre, Two-channel Kondo effect and renormalization flow with macroscopic quantum charge states, Nature (London) **526**, 233 (2015).
[26] A. Schiller and S. Hershfield, Exactly solvable nonequilibrium Kondo problem, Phys. Rev. B **51**, 12896 (1995).
[27] K. Majumdar, A. Schiller, and S. Hershfield, Nonequilibrium Kondo impurity: Perturbation about an exactly solvable point, Phys. Rev. B **57**, 2991 (1998).
[28] A. Oguri, Fermi-liquid theory for the Anderson model out of equlibrium, Phys. Rev. B **64**, 153305 (2001).
[29] A. Oguri, Out-of-equilibrium Anderson model at high and low bias voltage, J. Phys. Soc. Jpn. **74**, 110 (2005).
[30] A. C. Hewson, J. Bauer, and A. Oguri, Non-equilibrium differential conductance through a quantum dot in a magnetic field, J. Phys. Condens. Matter **17**, 5413 (2005).
[31] E. Sela and J. Malecki, Nonequilibrium conductance of asymmetric nanodevices in the Kondo regime, Phys. Rev. B **80**, 233103 (2009).
[32] M. Pletyukov and H. Schoeller, Nonequilibrium Kondo Model: Crossover from Weak to Strong Coupling, Phys. Rev. Lett. **108**, 260601 (2012).
[33] B. Doyon and N. Andrei, Universal aspects of nonequilibrium currents in a quantum dot, Phys. Rev. B **73**, 245326 (2006).
[34] J. Y. Yang, K. S. Yoon, Y. H. Do, C. O. Kim, J. P. Hong, Y. H. Rho, and H. J. Kim, Ferromagnetic quantum dots formed by external laser irradiation, J. Appl. Phys. **93**, 8766 (2003).
[35] L. Hofstetter, A. Geresdi, M. Aagesen, J. Nygård, C. Schönenberger, and S. Csonka, Ferromagnetic Proximity Effect in a Ferromagnet-Quantum-Dot-Superconductor Device, Phys. Rev. Lett. **104**, 246804 (2010).

[36] R. Delagrange, J. Basset, H. Bouchiat, and R. Deblock, Emission noise and high frequency cut-off of the Kondo effect in a quantum dot, arXiv:1704.00479.

[37] E. A. Alekseev, A. A. Belikov, R. V. Kozhynl, K. Schünemann, A. V. Shevchenko, D. M. Vavriv, V. A. Volkov, and V. V. Vynogradov, in *Proceedings of the 34th European Microwave Conference, Amsterdam, 2004* (IEEE, New York, 2004), p. 765.

[38] U. Meyer, G. Haack, C. Groth, and X. Waintal, Control of the Oscillatory Interlayer Exchange Interaction with Terahertz Radiation, Phys. Rev. Lett. **118**, 097701 (2017).

[39] I. Bloch, Ultracold quantum gases in optical lattices, Nature (London) **1**, 23 (2005).

[40] H. Zhang, Y. Zhai, and X. Chen, Spin dynamics in one-dimensional optical lattices, J. Phys. B **47**, 025301 (2014).

[41] S. Greschner and L. Santos, Anyon Hubbard Model in One-Dimensional Optical Lattices, Phys. Rev. Lett. **115**, 053002 (2015).

[42] M. Aidelsburger, M. Lohse, C. Schweizer, M. Atala, J. T. Barreiro, S. Nascimbène, N. Cooper, I. Bloch, and N. Goldman, Measuring the Chern number of Hofstadter bands with ultracold bosonic atoms, Nat. Phys. **11**, 162 (2015).

[43] J. S. Douglas, H. Habibian, C.-L. Hung, A. Gorshkov, H. J. Kimble, and D. E. Chang, Quantum many-body models with cold atoms coupled to photonic crystals, Nat. Photonics **9**, 326 (2015).

[44] P. Ponte, Z. Papić, F. Huveneers, and D. A. Abanin, Many-Body Localization in Periodically Driven Systems, Phys. Rev. Lett. **114**, 140401 (2015).

[45] A. Vogler, R. Labouvie, G. Barontini, S. Eggert, V. Guarrera, and H. Ott, Dimensional Phase Transition from an Array of 1D Luttinger Liquids to a 3D Bose-Einstein Condensate, Phys. Rev. Lett. **113**, 215301 (2014).

[46] A. Rapp, X. Deng, and L. Santos, Ultracold Lattice Gases with Periodically Modulated Interactions, Phys. Rev. Lett. **109**, 203005 (2012).

[47] T. Wang, X.-F. Zhang, F. E. A. dos Santos, S. Eggert, and A. Pelster, Tuning the quantum phase transition of bosons in optical lattices via periodic modulation of the *s*-wave scattering length, Phys. Rev. A **90**, 013633 (2014).